



1  
2  
3  
4  
5  
6  
7  
8  
9  
10  
11  
12  
13  
14  
15  
16  
17  
18  
19  
20  
21  
22  
23  
24  
25  
26  
27  
28  
29  
30  
31  
32

## Technical Note:

### **A note on stabilization mechanisms of, e.g., Atlantic Ocean meridional overturning circulation**

**by Hans van Haren**

Royal Netherlands Institute for Sea Research (NIOZ), P.O. Box 59, 1790 AB Den Burg,  
the Netherlands.  
e-mail: [hans.van.haren@nioz.nl](mailto:hans.van.haren@nioz.nl)



33 Short summary. The extent of mankind's influence on Earth's climate warrants ocean-studies.  
34 A supposed major heat-transporter is the Atlantic Meridional Overturning Circulation  
35 (AMOC). As AMOC is a complex nonlinear dynamical system, mathematical models may  
36 predict its potential collapse using single parameters like surface temperature. However,  
37 physical processes such as (sub-)mesoscale eddy transport and turbulent mixing by internal  
38 wave breaking will alter the estimators, so that the AMOC may not collapse.

39

40 **Abstract.** The extent of anthropogenic influence on the Earth's climate warrants studies of  
41 the ocean as a major player. The ocean circulation is important for transporting properties like  
42 heat, carbon and nutrients. A supposed major conduit is the Atlantic Meridional Overturning  
43 Circulation (AMOC). As the AMOC is a complex nonlinear dynamical system, it is  
44 challenging to predict its potential to collapse and/or reversal of direction from a statistical  
45 viewpoint using a single parameter like sea-surface temperature or freshwater influx in  
46 numerical models. However, as is argued in this note supported by spectra from ocean  
47 observations, physical processes such as transport by sub-mesoscale eddies and turbulence-  
48 generating breaking of internal waves that are not incorporated in these models will alter such  
49 parameters, and thereby statistical analyses. This may lead to feed-back mechanisms on  
50 property gradients such as density stratification so that the AMOC may not collapse.

51

## 52 **1 Introduction**

53 Schematically, the Atlantic(-Ocean) Meridional Overturning Circulation (AMOC)  
54 transports heat from the equator to the poles near the surface and carbon in the abyssal return  
55 (e.g., Aldama-Campino et al., 2023). It includes physical processes like 'deep dense-water  
56 formation' in the polar region. Recent mathematical and numerical modelling such as based  
57 on varying single parameters like sea-surface temperature (e.g., Ditlevsen and Ditlevsen,  
58 2023) and freshwater influx (e.g., van Westen et al., 2024) suggest a potential future collapse  
59 of the AMOC. It is argued that this may have consequences for Northwest-European climate.



60           Whilst the modelling might be robust mathematically, it lacks physical processes of  
61 the drivers of the AMOC and observational evidence thereof. This will have consequences for  
62 the feed-back mechanisms at work in the nonlinear dynamical system of ocean circulation. As  
63 has been reviewed for AMOC numerical models (Gent, 2018), important feed-back  
64 mechanisms are vertical (turbulent) mixing, (sub-)mesoscale gyre (eddy) transport, and the  
65 coupling with the atmosphere. Here we elaborate on the importance of turbulence induced by  
66 internal wave breaking, possibly coupling with sub-mesoscale eddies, and stability variations  
67 in vertical density stratification for such feed-back, by reviewing insights from recent  
68 modeling and deep-sea observations. In particular, the core of ocean motions is spectrally  
69 investigated focusing on most energetic mesoscale, internal wave, and turbulence scales.

70           In contrast with the atmosphere, the ocean is not a heat engine (Wunsch and Ferrari,  
71 2004). As a result, the AMOC is not buoyancy-driven via push by deep dense-water  
72 formation near the poles, which notably occurs in sporadic pulses rather than continuously.  
73 Instead, the AMOC is wind- and tide-driven, with turbulent mixing by internal wave breaking  
74 being considered an important physics process of pull. Winds, near the ocean surface, and  
75 tides, via interaction with seafloor topography deeper down, contribute about equally to  
76 generate internal waves that are found everywhere in the ocean interior. Such waves break  
77 predominantly at ubiquitous underwater seamounts and continental slopes.

78           Without turbulent mixing, the AMOC would be confined to a 100-m thick near-  
79 surface layer and the deep-ocean would be a stagnant pool of cold water (Wunsch and Ferrari,  
80 2004). This is not the case however, and the solar heat is mixed from the surface downward  
81 so that the ocean is stably stratified in density all the way into its deepest trenches, as has been  
82 shown in hydrographic deep-ocean observations (Taira et al., 2005; van Haren et al., 2021a).  
83 Although turbulent mixing by internal wave breaking in the ocean-interior is insufficient by at  
84 least a factor of two to maintain the vertical density stratification (e.g., Gregg, 1989, Polzin et  
85 al., 1997), such breaking along ocean boundaries has been suggested to be more than  
86 sufficient (Munk, 1966; Polzin et al., 1997). Especially large internal wave breaking is  
87 expected to occur above steeply sloping topography (Eriksen, 1982; Thorpe, 1987; Sarkar and



88 Scotti, 2017). Because there are more and larger seamounts than mountains on land, equally  
89 abundant sloping seafloors lead to abundant turbulent mixing, as has been charted from recent  
90 observations and modelling results summarized below.

91

## 92 **2 Recent internal wave breaking results**

93 Detailed observations and numerical modeling have revealed the extent of internal  
94 tide breaking processes above ocean topography (van Haren and Gostiaux, 2012; Winters,  
95 2015; Wynne-Cattanach et al., 2024). Quantification of the turbulent mixing shows that it  
96 occurs with typical tidal-period-average values that are more than 100 times larger over (just)  
97 super-critical slopes than open-ocean values. A super-critical seafloor slope is steeper than the  
98 slope of internal wave characteristics. While ocean-wide tides energetically dominate internal  
99 waves, not all seafloor slopes are super-critical for these waves. In contrast, nearly all seafloor  
100 slopes are super-critical for (at least one component of) secondly energetic near-inertial  
101 waves, which are generated via geostrophic adjustment following the passage or collapse of a  
102 disturbance such as fronts or atmospheric storms on the rotating Earth. Under common  
103 stratification, near-inertial waves are at the lowest frequency of freely propagating internal  
104 waves. The highest frequency propagating internal waves, near the buoyancy frequency,  
105 experience only vertical walls as super-critical seafloor slopes.

106 Within a tidal period, turbulence peaks in bursts of shorter duration than half an hour  
107 when highly nonlinear internal waves propagate as internal bores up a slope, once or twice a  
108 tidal cycle. The breaking of bores leads primarily to convective, buoyancy-driven turbulence,  
109 rather than frictional shear-turbulence over the seafloor (van Haren et al., 2013; van Haren et  
110 al., 2024). Between bores, the turbulent mixing varies by an order of magnitude in intensity,  
111 with effects extending about 100 m vertically and several kilometers horizontally from the  
112 seafloor. Although intermittently occurring at a given position of the sloping seafloor and  
113 about 10% varying in arrival time, the turbulence is generated internally by the tide, for about  
114 60% (Wunsch and Ferrari, 2004), and by winds, for about 40%, in a stratified ocean-



115 environment. The turbulent bores also resuspend sediment and thereby replenish nutrients  
116 away from the seafloor (Hosegood et al., 2004), important for deep-sea life.

117 Question is whether the intensity of internal-wave induced deep-ocean turbulence is  
118 affected by variations in sea-surface temperature or salinity, with what consequences for the  
119 AMOC. In considering these it should be noted that various properties determine different  
120 equilibria. For example, deep dense-water formation does not only occur in polar seas, but  
121 occasionally also in the at least 10°C warmer Mediterranean (Gascard, 1978), with an  
122 important contribution of atmospheric exchange due to orographic generated winds affecting  
123 the preconditioning by cooling and drying of near-surface waters. Similarly, internal waves  
124 occur in oceans and in the Mediterranean, but tides are relatively weak in the latter, and yet  
125 ‘sufficient’ turbulent mixing is generated via near-inertial motions mainly (van Haren et al.,  
126 2013).

127

### 128 **3 Revisiting Mediterranean observations as a proxy for ocean conditions**

129 In many physical oceanographic aspects of heat and salt budgets, large-scale water-  
130 flow circulation, eddies at sub-mesoscales, near-inertial motions including gyroscopic waves  
131 and internal wave turbulence, the Mediterranean Sea can be considered a sample for the state  
132 of the much larger oceans (e.g., Gascard, 1973; Garrett, 1994; Millot, 1999; van Haren and  
133 Millot, 2004; Testor and Gascard, 2006).

134 In the Northwest Mediterranean, vertical density stratification varies markedly with  
135 seasons and years, having relatively large near-surface values in summer and relatively low  
136 values in winter. The proximity of extensive mountain ranges on land generates highly  
137 variable winds that can cool and dry surface waters. In winter in weaker stratified waters, this  
138 may lead to unstable conditions of buoyancy driven convection in an exchange of dense-water  
139 sinking down, and less dense-waters up. Like in the polar regions, such exchange can be  
140 observed daily in the upper 10 m from the sea-surface, regularly down to a few 100 m from  
141 the surface, and seldom, once every 5-8 years (e.g., Rhein, 1995; Mertens and Schott, 1998),  
142 down to the abyssal seafloor at about 2500 m. In contrast, horizontal density gradients



143 associate with forcing of a dynamically unstable boundary current and eddies at multiple 1-  
144 100 km (sub-)mesoscales (e.g., Testor and Gascard, 2006). These eddy motions may push  
145 relatively warm waters down, thereby increasing the weak stratification in the deep-sea.

146 In summer, atmospheric disturbances are less intense, near-surface stratification is  
147 large due to solar heating, and eddy activity associated with some continental boundary flows  
148 is weaker (Albérola et al., 1995). This opens the possibility for detection of near-inertial wave  
149 dominance in kinetic energy. In relatively strong stratification, mainly gravity-driven parts of  
150 near-inertial waves generate largest vertical current differences ‘shear’ that destabilizes  
151 stratification due to their relatively short vertical length-scale, not only in the Mediterranean  
152 but also as observed in the Atlantic Ocean (van Haren, 2007). In near-homogeneous water-  
153 layers with weak stratification, their gyroscopic, Earth-rotation-driven, parts dominate and  
154 result in 0.1-1 km diameter sub-sub-mesoscale tubes of slantwise rather than vertical  
155 convection (Straneo et al., 2002; van Haren and Millot, 2004). Hence, one may expect  
156 frequency spectra of non-tidal dominated data from instruments moored in the Mediterranean  
157 reveal convection and thus deep transport under winter and summer conditions.

158 It is noted that ocean-spectra may show peaks such as at narrowband tidal and at,  
159 broader band, inertial frequencies, but they lack gaps. This lack of spectral gaps potentially  
160 couples motions at sub-inertial with inertial-buoyancy internal wave with super-buoyancy  
161 turbulence frequency ranges. However, it is unclear how such a coupling may work as some  
162 motions represent two-dimensional (2D) eddies, some linear waves, some non-linear waves,  
163 some anisotropic stratified turbulence, and some isotropic 3D turbulence.

164 Kinetic energy (KE) spectra from historic current meter observations down to mid-  
165 depth  $z = -1100$  m in the Ligurian Sea under upper-sea strongly stratified ‘summer’ and  
166 weakly stratified ‘winter’ conditions surely lack gaps (Fig. 1). Although these hourly sampled  
167 data barely resolve the turbulence ranges at frequencies higher than the buoyancy frequency,  
168 the internal wave continuum was suggested to scale with frequency  $\omega$  like  $\omega^p$ , with, on a log-



169 log plot, ‘spectral slope’  $p = -2.2 \pm 0.4$  (van Haren and Millot, 2003), independent of location  
170 and season albeit with different KE (power) levels.

171         Within the uncertainty range, several possible explanations can be given for the  
172 observed spectral slope. Internal gravity waves have been fitted to  $p = -2 \pm 0.5$  but only for  $f$   
173  $\ll \omega \ll N$  (Garrett and Munk, 1972), where  $f$  denotes the inertial frequency involving Earth  
174 rotation and  $N$  denotes the buoyancy frequency reflecting the square-root of vertical density  
175 stratification. Considering that the data in Fig. 1 are from a site where locally  $N = 3 \pm 2f$ ,  
176 irrespective of season (van Haren and Millot, 2003), alternative explanations were sought for  
177 observed spectral slopes at sub-inertial frequencies  $0.2 \text{ cpd} < \omega < f$ . Cpd is short for ‘cycles  
178 per day’. An obvious candidate is ‘fine-structure contamination’ of step functions passing  
179 sensors which gives a theoretical value of  $p = -2$  (Phillips, 1971; Reid, 1971). For their winter  
180 data, van Haren and Millot (2003) attributed such a slope to evidence intense mesoscale  
181 activity, because of the continuation of slope up to  $\omega = 5 \text{ cpd}$  before rolling off to white noise  
182 (slope 0). However, they did not elaborate. Below, the data in Fig. 1 are re-analyzed from a  
183 perspective of convection-turbulence.

184         Theoretical considerations of non-zero-mean flow convection-turbulence suggest a  
185 spectral scaling in the buoyancy range having  $p = -11/5 = -2.2$  for KE, and  $p = -7/5$  for a(n  
186 active) scalar quantity. This ‘BO’-scaling follows atmospheric and theoretical works by  
187 Bolgiano (1959) and Obukhov (1959). The scaling was set-up for a stably stratified  
188 (atmospheric) environment for the anisotropic part in which turbulent kinetic energy is  
189 partially transferred to potential energy leading to turbulent convection. Later works extended  
190 BO-scaling to purely buoyancy-driven turbulence, e.g. for Rayleigh-Bénard convection  
191 (Lohse and Xia, 2010).

192         Laboratory experiments on such gravitationally driven convection are inconclusive on  
193 BO-scaling. This scaling is confirmed for both KE and temperature in experiments by  
194 Ashkenazi and Steinberg (1999), while only for scalars by Pawar and Arakeri (2016) who  
195 found a slope of  $p = -5/3$  for KE. The  $p = -5/3$ -slope suggests dominance of shear-induced



196 turbulence of the inertial subrange for equilibrium (isotropic) turbulence cascade in the ‘KO’-  
197 scaling (Kolmogorov, 1941; Obukhov, 1949), but should also be found in spectra of scalars  
198 that are passive in this range. Obviously, scalars cannot be passive and active at the same time  
199 and space. This discrepancy between (types of) scaling between scalars and KE may be  
200 because the laboratory experiments of Pawar and Arakeri (2016) were in zero mean flow.  
201 Also, under sufficiently stable conditions without shear, no inertial subrange is expected  
202 (Bolgiano, 1959). However, the spectral extent of BO-scaling is largely unknown. While KO-  
203 scaling is based on a forward cascade of energy, the direction of energy cascade is  
204 inconclusive for BO-scaling and may be partially forward and partially backward, at least as  
205 reasoned for pure buoyancy-driven convection-turbulence (Lohse and Xia, 2010). Probably,  
206 directions of cascade change with locality in the flow, and perhaps depend on scale, which  
207 would also imply that KO- and BO-scaling cannot be found at the same site.

208 Revisiting data from non-zero mean flow and (weakly) stratified deep-sea in Fig. 1  
209 demonstrates the possibility of fit of  $p = -11/5$  outside near-inertial harmonic peaks. In winter,  
210 such a fit is observed consistently through the entire range of  $0.2 < \omega < 5$  cpd. In traditional  
211 terms, this frequency range covers the transition from mesoscale  $\omega < f$ , via internal wave  $f <$   
212  $\omega < N$ , to turbulence  $\omega > N$  motions. In summer, the  $p = -11/5$ -slope is found at two different  
213 KE levels for bands  $0.2 < \omega < \omega_{\min}$  and  $2\Omega < \omega < 5$  cpd at sub- and super-IGW frequencies,  
214 respectively. Here,  $\omega_{\min} < f$  denotes the minimum frequency bound for inertio-gravity waves  
215 IGW (LeBlond and Mysak, 1978) and  $\Omega$  the Earth rotational frequency. Maximum IGW is  
216 denoted by  $\omega_{\max} > 2\Omega$ . The plotted IGW-bounds  $[\omega_{\min} \omega_{\max}]$  are for weakly stratified, near-  
217 homogeneous layers in which  $N = f$ .

218 The bridge between the KE-levels at sub- and super-IGW is formed by the finitely  
219 broad near-inertial peak. The base of this peak is proposed to slope like  $p = -1$  reaching super-  
220 IGW BO-scaling at about  $\omega \approx 4$  cpd  $\approx N$ . Such  $p = -1$ -slope has been observed for the KE-  
221 spectral continuum between  $[f N]$  from the deep Bay of Biscay, Northeast Atlantic Ocean  
222 (van Haren et al., 2002). Theoretically, this slope represents spectral scaling of intermittency





223 of a weakly chaotic nonlinear system (Schuster, 1984), i.e., 3D dynamical systems that evolve  
224 into self-organized critical structures of states which are minimally stable (Bak et al., 1987).

225         These observations suggest a dominance of convection cascade from sub-meso- via  
226 IGW- to, probably because unresolved, turbulence-scales under high-energetic winter-  
227 conditions. It is also observed under quieter summer conditions when, however, such a  
228 cascade is masked by IGW that lead a cascade at  $\omega > \omega_{\min}$ . Especially the sub-inertial range of  
229 apparent BO-scaling seems out of the turbulence range, unless waters are near-homogeneous  
230  $N \rightarrow 0$  so that  $\omega_{\min} \rightarrow 0$ . This would extend not only IGW, notably gyroscopic waves, but  
231 also turbulence, probably in the form of slantwise convection, to the (sub-)mesoscale range.

232         For the mesoscale range, the observations in Fig. 1 are supported by numerical  
233 modeling results that have suggested eddy-KE has a broad range of spectral slopes between  $-3$   
234  $< p < -5/3$  (Storer et al., 2022), and by satellite altimetry observations that indicated, after  
235 noise-correction and transfer to KE, a best-fit of  $p = -2.28$  (Xu and Fu, 2012). No mention  
236 was made of BO-scaling, but the correspondence seems evident.

237         As the KE in Fig. 1 is at least one order of magnitude larger in winter than in  
238 summer, a near-inertial peak, if existent, will be part of the spectral continuum during the  
239 former. Saint-Guilly (1972) proposed that winter-time inertial KE is spread over a broad  
240 featureless band, like quasi-gyroscopic waves may be present between IGW-bounds [ $\omega_{\min}$ ,  
241  $\omega_{\max}$ ] for  $N \sim f$  (LeBlond and Mysak, 1978; Gerkema et al., 2008). However, observations  
242 from the year-round upper-layer-stratified central Western Mediterranean demonstrate that,  
243 also in deep homogeneous  $N = 0$  waters, a near-inertial peak is observed in KE-spectra (van  
244 Haren and Millot, 2004). This may be attributed to a year-round source of atmospheric-  
245 generated inertial waves that are the only internal waves that can propagate without reflection  
246 from well-stratified to near-homogeneous layers and back (van Haren, 2023b).

247         Based on limited spectral observations, Gascard (1973) suggested the generation of  
248 12-h stability waves (close to the buoyancy frequency of very weak stratification) that may  
249 briefly force dense-water formation, thereby implicitly suggesting a link between internal



250 waves and (sub-)mesoscale eddies. As such eddies have estimated relative vorticity of  $|\zeta| = f/2$   
251 in the Western Mediterranean (Testor and Gascard, 2006), this addition to the planetary  
252 vorticity ( $f$ ) automatically widens the ‘effective’ near-inertial band  $0.5f < f_{\text{eff}} < 1.5f$ , which  
253 bounds are close to IGW-bounds for  $N = 0.8f$ . One of the properties can be a modification of  
254 near-inertial frequency (Perkins, 1976), and trapping of near-inertial waves in anticyclonic  
255 eddies (Kunze, 1985). Although found to be limited to the rather flat KE-spectral dip in the  
256 immediate half-order-of-magnitude sub-inertial frequency band, standing vortical modes  
257 (low-frequency non-propagating motions) of vertical length-scale  $< 10$  m are suggested to be  
258 as energetic as internal waves (Polzin et al., 2003). Alternatively, it has been suggested for  
259 North-Atlantic observations that vortical modes may interact with internal waves, affecting  
260 internal-wave shear that was peaking over  $O(10)$  m vertical scales at IGW-frequencies in a  
261 band with limits determined by weak stratification as in  $N = f$  (van Haren, 2007).

262 For hypothetical  $\omega_{\text{min}} = 0.2$  cpd, at which the observed spectral slope changes away  
263 from  $p = -11/5$  (Fig. 1), one would require  $N = 0.21f$ , which is almost unmeasurable and not  
264 existent for any prolonged period even in the deep Northwestern Mediterranean, to the  
265 knowledge of the author. However, it may reflect  $\omega_{\text{min}}$  computed using  $f_{\text{eff}} = 0.5f$  and  $N = f_{\text{eff}}$ ,  
266 noting that such conditions can only apply for part of the record. If so, it would reflect a direct  
267 coupling between sub-mesoscale and IGW-motions with slantwise convection (Straneo et al.,  
268 2002; van Haren and Millot, 2004; Gerkema et al., 2008). The  $p = -11/5$  is significantly  
269 distinguishable from  $-2$  over a frequency range of nearly two orders of magnitude, and from  $-$   
270  $5/3$  over a range of just over half an order of magnitude (Fig. 1). The roll-off to noise (slope  
271  $0$ ), for  $\omega > 5$  cpd, may partially be seen as following a slope of  $p = -5/3$  before  $0$ . The roll-off  
272 around  $0.1$  cpd suggests an unresolved broad mesoscale peak-value between  $0.01$  and  $0.1$  cpd.  
273 While these 1980’s moored current meter data barely resolved the turbulence part of the KE-  
274 spectrum, their temperature sensors were too poor to simultaneously verify any spectral  
275 scaling for scalars.



276 About 40 years later, high-resolution moored temperature sensor ‘‘T-’ data provided  
277 opportunity to verify scalar spectral scaling in the area. These T-data evidenced occasional  
278 warming of the deep Northwest Mediterranean seafloor (Fig. 2a), which, after comparison  
279 with data from higher-up appeared to be coming from above, or slanted sideways, under  
280 relatively stratified conditions (van Haren, 2023a). The data were collected during mid-fall,  
281 when waters above were sufficiently stratified and no (cooler) dense-water convection was  
282 formed. The broad two-day warming around day 308 is most stratified, whilst during other  
283 periods waters are only weakly stratified, including the quasi-inertial variations between days  
284 316 and 322. These weakly stratified near-inertial, or near-buoyancy as  $N \approx f$ , temperature  
285 variations may evidence slantwise quasi-gyroscopic near-inertial waves, which can have a  
286 large vertical component (LeBlond and Mysak, 1978), as opposed to more common near-  
287 horizontal near-inertial waves in strongly stratified waters that are barely noticeable in  
288 temperature records.

289 The 18-day average spectra of the 2-s sampled data poorly resolve sub-mesoscales,  
290 but show a well-resolved slope of  $p = -1.4 \pm 0.025$  between  $0.5 < \omega < 6000$  cpd, across the  
291 IGW band and well into the turbulence band (Fig. 2b). No transition to a  $-5/3$ -slope is  
292 observed before roll-off to noise. The observed  $p = -7/5$ -slope is found significantly different  
293 from  $p = -2$  and  $-5/3$  over the indicated frequency range of four orders of magnitude and over  
294 the turbulence range between  $100 < \omega < 10^4$  cpd. Over a frequency range of half an order of  
295 magnitude the slope-error is about  $\pm 0.1$ . Albeit not greatly resolved, the range between  $\omega_{\max} <$   
296  $\omega < 10$  cpd falls-off steeper roughly at  $p = -2$  and the range between  $10 < \omega < 100$  cpd shows  
297 a reduced variance that may partially be characterized by intermittency ( $p = -1$ ; Schuster,  
298 1984), but which is not yet explained. Here, it is observed to bridge between  $p = -2$  and super-  
299 IGW BO-scaling  $p = -7/5$ . This would be further observation of a marginally ocean-state to  
300 the  $-1$ -scaling in KE-spectra (present Fig. 1 and van Haren et al., 2002) and in the continuum  
301 of the band  $[f N]$  in open-ocean T-spectra (van Haren and Gostiaux, 2009).



302           Whilst more extended work with longer data sets is to be done, these high-resolution  
303 temperature observations suggest a direct coupling between sub-mesoscale motions, IGW  
304 motions, comprising internal gravity and gyroscopic waves, and convection turbulence. The  
305 temperature spectra are also consistent with the limited KE-spectra of Fig. 1 from roughly the  
306 same area, and both indicate a dominance of non-isotropic, stratified-turbulence convection  
307 between sub-mesoscales and largest turbulent overturning scales in extended BO-scaling  
308 suggesting cross-spectral coupling. The discrepancy with KE-spectra in laboratory  
309 experiments of Pawar and Arakeri (2016) may be due to difference of settings. In a non-zero  
310 mean flow turbulence convection experiment near the gas-liquid critical point, BO-scaling  
311 was observed for both KE and temperature (Ashkenazi and Steinberg, 1999). We recall that  
312 our deep-sea conditions are non-zero mean flow, weak tides, very high bulk Reynolds  
313 numbers  $O(10^5)$  given the large scales, and varying non-zero vertical density stratification.

314           The mesoscale-IGW-turbulence motions transport and mix warm waters downward.  
315 This contrasts with the process of buoyancy-driven dense-water formation that is thought to  
316 bring cooler waters downward during short periods of time, but for which no evidence exists  
317 in the 18-day T-sensor data set.

318

#### 319 **4 How robust is the system of ocean circulation and stratification?**

320           Any variation to the nonlinear system of ocean circulation may encounter several  
321 complex feedback mechanisms, of which the effects are not yet fully understood for the  
322 present-day ocean. Although stable density stratification hampers vertical exchange by  
323 turbulent mixing, it does not block it. While stratification supports internal waves and their  
324 destabilizing shear, turbulent mixing during particular phase of a wave may decrease or  
325 destroy it locally in time and space. However, a subsequent internal wave-phase will restratify  
326 the mixed patch, thereby maintaining its own support of stable stratification. Such a feed-back  
327 system may be at work, for example when the ocean absorbs more heat.

328           Increased sea-surface temperature may lead to increased vertical density  
329 stratification, which may lead to less turbulent exchange as vertical overturning is suppressed.



330 However, it will also lead to more internal waves through the extension of their spectral band  
331 to higher frequencies, with the potential to increased interaction, non-linearity, and  
332 turbulence-generating wave breaking. As particular internal waves can propagate deep into  
333 the ocean interior, they can cause enhanced turbulent mixing elsewhere.

334 Limited observations have thus far not provided evidence for an inverse  
335 correspondence between changes in turbulent mixing and changes in temperature across the  
336 near-surface photic zone along a longitudinal section of the Northeast Atlantic Ocean (van  
337 Haren et al., 2021b). This lack of correspondence suggests a feedback mechanism at work  
338 mediating potential physical environment changes so that global warming may not affect  
339 vertical turbulent fluxes of heat, and thereby also of, e.g., carbon. One such feedback  
340 mechanism may be convection-turbulence induced by internal waves and sub-mesoscale  
341 eddies. Re-analysis of moored current meter data from the Irminger Sea (North-Atlantic  
342 Ocean) demonstrate a significant  $p = -11/5$  spectral slope at sub- and at super-inertial  
343 frequencies (Fig. 3). As was outlined in van Haren (2007), the area showed an IGW-band (for  
344  $N = f$ ) with dominant sub-inertial shear at small 8-m vertical scales despite the dominant  
345 internal tidal KE. The correspondence with the Mediterranean data of Fig. 1 is striking,  
346 including the one order of magnitude change in KE between sub- and super-IGW  $p = -11/5$ -  
347 slopes with similar  $p = -1$  bridge albeit uncertain crossing level, and similar heights of near-  
348 inertial peak despite the tidal peak in Fig. 3.

349 While few ocean observations have been presented of BO-scaling thus far, coupling  
350 has not been established between convection and stratified small-scale turbulence with  
351 mesoscale motions. Likewise, complexing factors are spectral interruption by internal waves.  
352 However, internal wave trapping by mesoscale eddies has been well described (e.g., Kunze,  
353 1985), and which thus provides an obvious coupling between these motions. It is expected  
354 that such coupling may lead to strong nonlinearity (of the internal waves) that leads to  
355 turbulent mixing produced by wave breaking.

356 As demonstrated using Mediterranean observations, not only convectively unstable  
357 cooler and/or saltier waters potentially lead to downward motions from the surface. Also sub-



358 mesoscale eddies and near-inertial waves can convectively push stratified waters to the deep  
359 sea. Such downward push can be fast to transport materials from surface to 2500-m deep  
360 seafloor in a day (van Haren et al., 2006), and which speed is of the same order of magnitude  
361 as attributed to dense-water convection (Schott et al., 1996). It can also be more turbulent  
362 compared to shear-induced motions in the stratified ocean-interior, whereby turbulence  
363 reaches the seafloor according to few observations from the abyssal Pacific (van Haren, 2020)  
364 and alpine freshwater Lake Garda (van Haren and Dijkstra, 2021). Further extended  
365 observational evidence is urgently needed.

366         Although the anthropogenic influence on the Earth's climate is without doubt, the  
367 impact on the ocean circulation is not fully known because we lack sufficient, notably  
368 observational, information of the relevant processes that can thus not be properly modeled  
369 yet. Therefore, we should be cautious in making predictions such as in (e.g., Ditlevsen and  
370 Ditlevsen, 2023; van Westen et al., 2024) on future ocean circulation based on single  
371 parameters like ocean-surface temperature or fresh-water flux that are uncertain proxies.  
372 Because no observational (van Haren et al., 2021b), modeling (Little et al., 2020) or paleo-  
373 proxy validation (Cisneros et al., 2019) physics evidence exists that sea-surface temperature is  
374 a solid estimator of AMOC-strength variations, other properties like vertical density gradients  
375 (stratification), and turbulence intensity may be considered.

376         Variability of the ocean in space and time is a key to its dynamics, but it is unclear  
377 how robust such variations can be, e.g., whether shifting sites for deep dense-water formation  
378 (Gou et al., 2024) may be part of the same system. Observational evidence verifying  
379 numerical simulations' outcome, not only predictions but also present-day, of ocean-state is  
380 needed. Observations are also required to evidence variability in relevant physics processes  
381 for model-implementation. Besides eddies and coupling with atmosphere (e.g., Gent, 2018),  
382 numerical models of complex nonlinear ocean circulation should contain internal-wave  
383 turbulence with appropriate space and time dependency.

384         As for the ocean circulation in the horizontal plane near its surface with most impact on  
385 mankind, wind will remain the main driver rather than the AMOC. As long as the Earth



386 rotation does not alter direction, wind will maintain its general course (Wunsch, 2004). The  
387 atmosphere remains the key player in the global heat transport across mid-latitudes rather than  
388 the ocean. Simultaneously, the importance of processes like stratification and turbulent  
389 mixing induced by, e.g., internal wave breaking with or without sub-mesoscale coupling  
390 cannot be underestimated for life near the ocean-surface as well as in the -deep, because it  
391 will come to a halt without such processes.

392

393 *Data availability.* No new data were created or analyzed in this study: replot and re-analysis  
394 of data presented in van Haren and Millot (2003), in van Haren (2007) and in van Haren  
395 (2023a).

396

397 *Competing interests.* The author declares that he has no conflict of interest.

398

399 *Acknowledgments.* I thank L. Gerringa for commenting a previous draft of the manuscript.

400



401 **References**

- 402 Albérola, C., Millot, C., and Font, J.: On the seasonal and mesoscale variabilities of the  
403 Northern Current during the PRIMO-0 experiment in the western Mediterranean Sea.  
404 *Oceanol. Acta*, 18, 163-192, 1995.
- 405 Aldama-Campino A., Fransner F., Ödalen, M., Groeskamp, S., Yool, A. Döös, K., and  
406 Nycander, J.: Meridional ocean carbon transport, *Global Biogeochem. Cy.*, 34  
407 e2029GB006336, 2023.
- 408 Ashkenazi, S., and Steinberg, V.: Spectra and statistics of velocity and temperature  
409 fluctuations in turbulent convection, *Phys. Rev. Lett.*, 83, 4760-4763, 1999.
- 410 Bak, P., Tang, C., and Wiesenfeld, K.: Self-organized criticality: An explanation of the  $1/f$   
411 noise, *Phys. Rev. Lett.*, 59, 381-384, 1987.
- 412 Bolgiano, R.: Turbulent spectra in a stably stratified atmosphere, *J. Geophys. Res.*, 64, 2226-  
413 2229, 1959.
- 414 Cisneros, M., Cacho, I., Frigola, J., Snchez-Vidal, A., Calafat, A., Pedrosa-Pàmies, R.,  
415 Rumín-Caparrós, A., and Canals, M.: Deep-water formation variability in the north-  
416 western Mediterranean Sea during the last 2500 yr: A proxy validation with present-day  
417 data, *Glob. Planet. Chang.* 177, 56-68, 2019.
- 418 Ditlevsen, P., and Ditlevsen, S.: Warning of a forthcoming collapse of the Atlantic meridional  
419 overturning circulation, *Nat. Comm.* 14, 4254, 2023.
- 420 Eriksen, C. C.: Observations of internal wave reflection off sloping bottoms, *J. Geophys.*  
421 *Res.*, 87, 525-538, 1982.
- 422 Garrett, C.: The Mediterranean Sea as a climate test basin, In: Malanotte-Rizzoli, P., and  
423 Robinson, A. R. eds., *Ocean Processes in Climate Dynamics: Global and Mediterranean*  
424 *Examples*, Kluwer Academic Publishes, 227-237, 1994.
- 425 Garrett, C., and Munk, W.: Space-time scales of internal waves, *Geophys. Fluid Dyn.*, 3, 225-  
426 264, 1972.





- 427 Gascard, J.-C.: Vertical motions in a region of deep water formation, *Deep-Sea Res.*, 20,  
428 1011-1027, 1973.
- 429 Gascard, J.-C.: Mediterranean deep water formation, baroclinic eddies and ocean eddies,  
430 *Oceanol. Acta*, 1, 315-330, 1978.
- 431 Gent, P. R.: A commentary on the Atlantic meridional overturning circulation stability on  
432 climate models, *Ocean Mod.*, 122, 57-66, 2018.
- 433 Gerkema, T., Zimmerman, J. T. F., Maas, L. R. M., and van Haren, H.: Geophysical and  
434 astrophysical fluid dynamics beyond the traditional approximation, *Rev. Geophys.*, 46,  
435 RG2004, doi:10.1029/2006RG000220, 2008.
- 436 Gou, R., Wang, Y., Xiao, K., and Wu, L.: A plausible emergence of new convection sites in  
437 the Arctic Ocean in a warming climate, *Environ. Res. Lett.*, 19, 031001, 2024.
- 438 Gregg, M. C.: Scaling turbulent dissipation in the thermocline, *J. Geophys. Res.*, 94, 9686-  
439 9698, 1989.
- 440 Hosegood, P., Bonnin, J., and van Haren, H.: Solibore-induced sediment resuspension in the  
441 Faeroe-Shetland Channel, *Geophys. Res. Lett.*, 31, L09301, doi:10.1029/2004GL019544,  
442 2004.
- 443 Kolmogorov, A. N.: The local structure of turbulence in incompressible viscous fluid for very  
444 large Reynolds numbers, *Dokl. Akad. Nauk SSSR*, 30, 301-305, 1941.
- 445 Kunze, E.: Near-inertial wave propagation in geostrophic shear, *J. Phys. Oceanogr.*, 15, 544-  
446 565, 1985.
- 447 LeBlond, P. H., and Mysak, L. A.: *Waves in the ocean*, Elsevier, New York, 602 pp., 1978.
- 448 Little, C. M., Zhao, M., and Buckley, M. W.: Do surface temperature indices reflect  
449 centennial-timescale trends in Atlantic Meridional Overturning Circulation strength?  
450 *Geophys. Res. Lett.*, 47, e2020GL090888, 2020.
- 451 Lohse, D., and Xia, K.-Q.: Small-Scale properties of turbulent Rayleigh-Bénard convection,  
452 *Annu. Rev. Fluid Mech.*, 42, 335-364, 2010.
- 453 Mertens, C., and Schott, F.: Interannual variability of deep-water formation in the  
454 Northwestern Mediterranean, *J. Phys. Oceanogr.*, 28, 1410-1424, 1998.



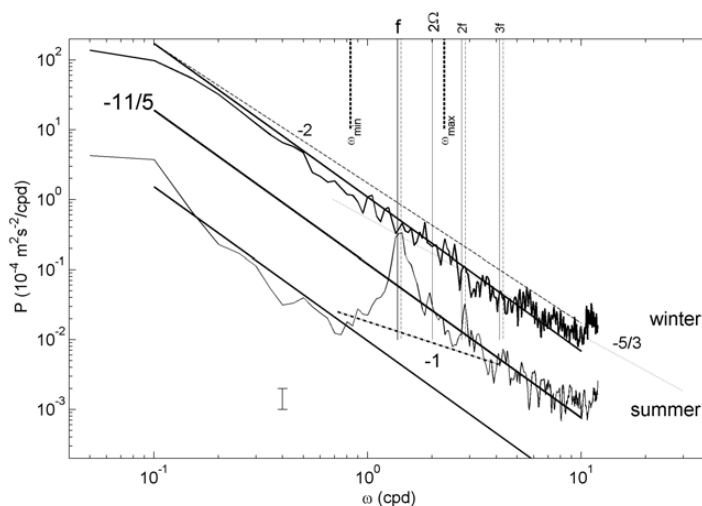
- 455 Millot, C.: Circulation in the Western Mediterranean Sea, *J. Mar. Sys.*, 20, 423-442, 1999.
- 456 Munk, W.: Abyssal recipes, *Deep-Sea Res.*, 13, 707-730, 1966.
- 457 Obukhov, A. M.: Structure of the temperature field in a turbulent flow, *Izv. Akad. Nauk*  
458 *SSSR, Ser. Geogr. Geofiz.*, 13, 58-69, 1949.
- 459 Obukhov, A. M.: Effect of buoyancy forces on the structure of temperature field in a turbulent  
460 flow, *Dokl. Akad. Nauk SSSR*, 125, 1246-1248, 1959.
- 461 Pawar, S. S., and Arakeri, J. H.: Kinetic energy and scalar spectra in high Rayleigh number  
462 axially homogeneous buoyancy driven turbulence, *Phys. Fluids*, 28, 065103, 2016.
- 463 Perkins, H.: Observed effect of an eddy on inertial oscillations, *Deep-Sea Res.*, 23, 1037-  
464 1042, 1976.
- 465 Phillips, O. M.: On spectra measured in an undulating layered medium, *J. Phys. Oceanogr.*, 1,  
466 1-6, 1971.
- 467 Polzin, K. L., Toole, J. M., Ledwell, J. R., and Schmitt, R. W.: Spatial variability of turbulent  
468 mixing in the abyssal ocean, *Science*, 276, 93-96, 1997.
- 469 Polzin, K. L., Kunze, E., Toole, J. M., and Schmitt, R. W.: The partition of finescale energy  
470 into internal waves and subinertial motions, *J. Phys. Oceanogr.*, 33, 234-248, 2003.
- 471 Reid, R. O.: A special case of Phillips' general theory of sampling statistics for a layered  
472 medium, *J. Phys. Oceanogr.*, 1, 61-62, 1971.
- 473 Rhein, M.: Deep water formation in the western Mediterranean, *J. Geophys. Res.*, 100, 6943-  
474 6959, 1995.
- 475 Saint-Guilly, B.: On the response of the ocean to impulse, *Tellus* 24, 344-349, 1972.
- 476 Sarkar, S., and Scotti, A.: From topographic internal gravity waves to turbulence, *Ann. Rev.*  
477 *Fluid Mech.*, 49, 195-220, 2017.
- 478 Schott, F., Visbeck, M., Send, U., Fischer, J., and Desaubies, Y.: Observations of deep  
479 convection in the Gulf of Lions, Northern Mediterranean, during the winter of 1991/92, *J.*  
480 *Phys. Oceanogr.*, 26, 505-524, 1996.
- 481 Schuster, H. G., *Deterministic Chaos: An Introduction*, Physik-Verlag, Weinheim, 220 pp.,  
482 1984.



- 483 Storer, B. A., Buzzicotti, M., Khatri, H., Griffies, S. M., and Aluie, H.: Global energy  
484 spectrum of the general oceanic circulation, *Nat. Comm.*, 13, 5314, 2022.
- 485 Straneo, F., Kawase, M., and Riser, S. C.: Idealized models of slantwise convection in a  
486 baroclinic flow, *J. Phys. Oceanogr.*, 32, 558-572, 2002.
- 487 Taira, K., Yanagimoto D., and Kitagawa, S.: Deep CTD casts in the challenger deep. Mariana  
488 Trench, *J. Oceanogr.*, 61, 447-454, 2005.
- 489 Testor, P., and Gascard, J.C.: Post-convection spreading phase in the Northwestern  
490 Mediterranean Sea, *Deep-Sea Res.*, 53, 869-893, 2006.
- 491 Thorpe, S. A.: Transitional phenomena and the development of turbulence in stratified fluids:  
492 a review, *J. Geophys. Res.*, 92, 5231-5248, 1987.
- 493 van Haren, H.: Inertial and tidal shear variability above Reykjanes Ridge, *Deep-Sea. Res. I*,  
494 54, 856-870, 2007.
- 495 van Haren, H.: Slow persistent mixing in the abyss, *Ocean Dyn.*, 70, 339-352, 2020.
- 496 van Haren, H.: Convection and intermittency noise in water temperature near a deep  
497 Mediterranean seafloor, *Phys. Fluids*, 35, 026604, 2023a.
- 498 van Haren, H.: Near-inertial wave propagation between stratified and homogeneous layers, *J.*  
499 *Oceanogr.*, 79, 367-377, 2023b.
- 500 van Haren, H., and Dijkstra, H. A.: Convection under internal waves in an alpine lake, *Env.*  
501 *Fluid Mech.*, 21, 305-316, 2021.
- 502 van Haren, H., and Gostiaux, L.: High-resolution open-ocean temperature spectra, *J.*  
503 *Geophys. Res.*, 114, C05005, doi:10.1029/2008JC004967, 2009.
- 504 van Haren, H., and Gostiaux, L.: Detailed internal wave mixing observed above a deep-ocean  
505 slope, *J. Mar. Res.*, 70, 173-197, 2012.
- 506 van Haren, H. and Millot, C.: Seasonality of internal gravity waves kinetic energy spectra in  
507 the Ligurian Basin, *Oceanol. Acta*, 26, 635-644, 2003.
- 508 van Haren, H., and Millot, C.: Rectilinear and circular inertial motions in the Western  
509 Mediterranean Sea, *Deep-Sea Res. I*, 51, 1441-1455, 2004.

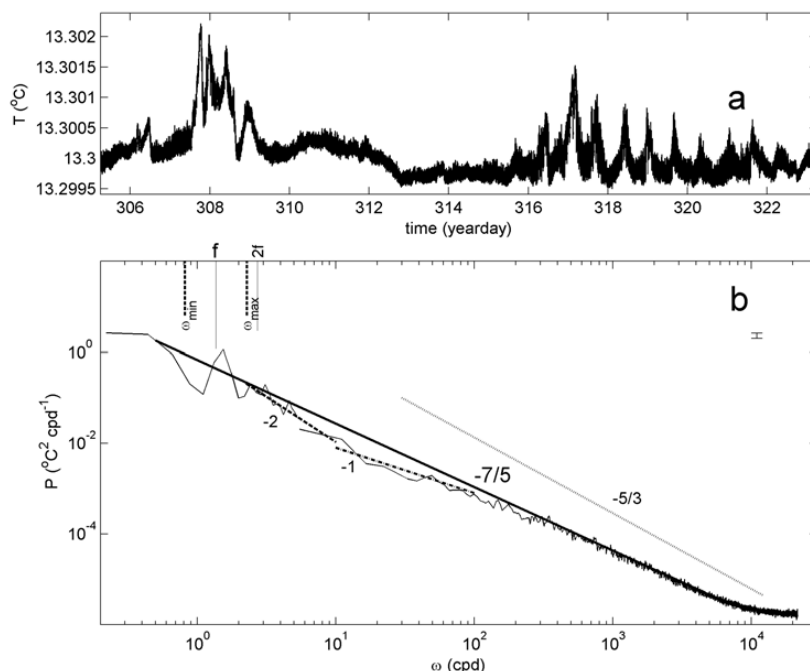


- 510 van Haren, H., Maas, L., and van Aken, H.: On the nature of internal wave spectra near a  
511 continental slope, *Geophys. Res. Lett.*, 29(12), 10.1029/2001GL014341, 2002.
- 512 van Haren, H., Millot, C., and Taupier-Letage, I.: Fast deep sinking in Mediterranean eddies,  
513 *Geophys. Res. Lett.*, 33, L04606, doi:10.1029/2005GL025367, 2006.
- 514 van Haren, H., Ribó, M., and Puig, P.: (Sub-)inertial wave boundary turbulence in the Gulf of  
515 Valencia. *J. Geophys. Res.Oceans*, 118, 2067-2073, doi:10.1002/jgrc.20168, 2013.
- 516 van Haren, H., Uchida, H., and Yanagimoto, D.: Further correcting pressure effects on  
517 SBE911 CTD-conductivity data from hadal depths, *J. Oceanogr.*, 77, 137-144, 2021a.
- 518 van Haren, H., Brussaard, C. P. D., Gerringa, L. J. A., van Manen, M. H., Middag, R., and  
519 Groenewegen, R.: Diapycnal mixing near the photic zone of the NE-Atlantic, *Ocean Sci.*,  
520 17, 301-318, 2021b.
- 521 van Haren, H., Voet, G., Alford, M. H., Fernandez-Castro, B., Naveira Garabato, A. C.,  
522 Wynne-Cattanach, B. L., Mercier, H., and Messias, M.-J.: Near-slope turbulence in a  
523 Rockall canyon, *Deep-Sea Res. I*, 206, 104277, 2024.
- 524 van Westen, R. M., Kliphuis, M., and Dijkstra, H.A.: Physics-based early warning signal  
525 shows that AMOC is on tipping course, *Sci. Adv.*, 10, eadk1189, 2024.
- 526 Winters, K. B.: Tidally driven mixing and dissipation in the stratified boundary layer above  
527 steep submarine topography, *Geophys. Res. Lett.*, 42, 7123-7130, 2015.
- 528 Wunsch, C.: Gulf Stream safe if wind blows and Earth turns, *Nature*, 428, 601, 2004.
- 529 Wunsch, C., and Ferrari, R.: Vertical mixing, energy and the general circulation of the oceans,  
530 *Ann. Rev. Fluid Mech.*, 36, 281-314, 2004.
- 531 Wynne-Cattanach, B. L., Couto, N., Drake, H. F., Ferrari, R., Le Boyer, A., Mercier, H.,  
532 Messias, M.-J., Ruan, X., Spingys, C. P., van Haren, H., Voet, G., Polzin, K., Naveira  
533 Garabato, A., and Alford, M. H.: Observational evidence of diapycnal upwelling within a  
534 sloping submarine canyon, *Nature*, 630, 884-890, 2024.
- 535 Xu, Y., and Fu, L.-L.: The effects of altimeter instrument noise on the estimation of the  
536 wavenumber spectrum of sea surface height, *J. Phys. Oceanogr.*, 42, 2229-2233, 2012.

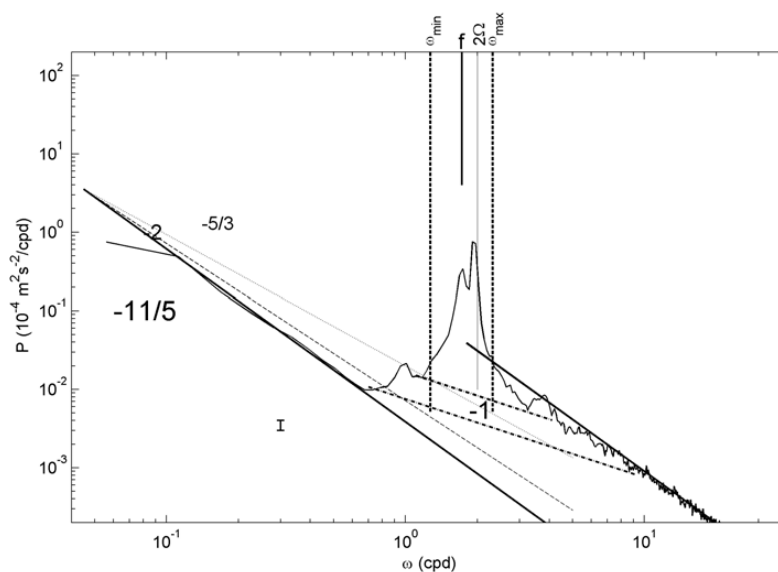


537

538 **Fig. 1.** Moderately smoothed (20 degrees of freedom, dof) kinetic energy (KE) spectra over  
 539 100 days of data from 600-s sampled Aanderaa mechanical current meter moored in  
 540 1981/1982 at  $z = -1100$  m over the continental slope in the Ligurian Sea at  $43^\circ 28.32' N$ ,  $7^\circ$   
 541  $46.10' E$ , 2250 m water depth. For details on these data, see van Haren and Millot (2003). The  
 542 ‘summer’ spectrum is an average from data between days 190 and 290 (in 1981), the ‘winter’  
 543 between days 375 and 475 (adding +365 for days in 1982). Several frequencies are indicated  
 544 including inertial frequency  $f$ , Earth rotational  $\Omega$  and inertio-gravity wave bounds [ $\omega_{\min} < f$ ,  
 545  $\omega_{\max} > N$ ] for buoyancy frequency  $N = f$ . The dashed lines indicate (harmonics of)  $1.04f$ . Four  
 546 spectral slopes  $\omega^p$  are indicated by their exponent:  $p = -11/5$  (solid slope in the log-log plot)  
 547 for Bolgiano-Obukhov ‘BO’ scaling reflecting the buoyancy subrange of convective  
 548 turbulence (e.g., Pawar and Arakeri, 2016),  $p = -5/3$  (dotted slope) for Kolmogorov-Obukhov  
 549 ‘KO’ scaling reflecting the equilibrium inertial subrange for dominant shear-induced  
 550 turbulence (Kolmogorov 1941; Obukhov, 1949),  $p = -1$  (dash-dotted slope) for intermittency  
 551 of self-organized criticality (Schuster, 1984; Bak et al., 1987) and  $p = -2$  (dashed slope) for  
 552 internal wave scaling (Garrett and Munk, 1972) or finestructure contamination (Phillips,  
 553 1971; Reid, 1971).



554  
555 **Fig. 2.** Eighteen days of high-resolution 2-s sampled temperature ( $T$ ) data from a NIOZ  
556  $T$ -sensor fallen off a mooring-line in 2020, and lying 0.01 m above a flat seafloor about  
557 10 km south of the foot of the continental slope at  $42^\circ 49.50' N$ ,  $6^\circ 11.78' E$ , 2458 m  
558 water depth, about 100 km WSW from the site in Fig. 1. For details on these data see van  
559 Haren (2023a). (a) Time series of 18 days of raw temperature data. (b) Weakly smoothed  
560 (10 dof;  $\omega < 5$  cpd) and heavily smoothed (250 dof;  $\omega > 5$  cpd) temperature variance spectra  
561 of data in a. Frequency and spectral slope indications as in Fig. 1, while  $-7/5$  (solid slope)  
562 indicates BO-scaling of an active scalar (e.g. Pawar and Arakeri, 2016), and  $-1$  (dash-  
563 dotted slope) for scaling of intermittency of a weakly chaotic nonlinear system (Schuster,  
564 1984). Note the different axes-ranges compared with Fig. 1.



565  
566 **Fig. 3.** Like Fig. 1, but for strongly smoothed (50 dof) KE spectra averaged over 400 days  
567 of data from 600-s sampled Valeport mechanical current meter moored at  $z = -1000$  m  
568 over the Mid-Atlantic Ridge at  $58^\circ 59.67' \text{ N}$ ,  $33^\circ 56.12' \text{ W}$ , 2540 m water depth in  
569 2003/2004, within the project discussed in van Haren (2007).  
570